Automatic determination of arterial input function for estimating tumor microvessel density with dynamic contrast-enhanced MRI in mice model

J-H. Kim[1], G-H. Im[2], J. Yang[1], and J. Lee[1]
[1]Department of Radiology, Samsung Medical Center, Seoul, Gang-Name, Korea, Republic of, [2]Center for Molecular and Cellular Imaging, Samsung Biomedical Research Institute, Samsung Medical Center, Seoul, Korea, Republic of

Introduction

Recently, application of DCE-MRI has gained increasing attention for use in drug development in pre-clinical research using mouse models, especially for assessment of angiogenesis for anti-angiogenic drug development (*1*). In the mouse, the AIF has been manually measured from a large arterial vessel in the center of the left heart ventricle (*2*). In this case, when the tumor is far from the heart, the MRI acquisition needs unnecessarily large FOV selection which results in an increasing acquisition time. In addition, this manual detection procedure is time consuming and subjective, depending on the operators' experience. Moreover, manual AIF measurement in MR images of mice is often difficult due to small spatial dimensions, motion effects, or location of tumors. Nevertheless, an algorithm for automatic detection of AIF specific for small animals, such as mice or rats, has not yet been developed. In this study, we propose a new method for automatic detection of AIF that can effectively be used for mice data.

Methods

Acquisition of MR Data: For a subcutaneous xenograft tumor model, ectopic xenograft tumors were established by subcutaneous injection of 2×10^6 SKOV3 cells into the right thigh in 8 male BALB/c nude mice (7 weeks old). All MRI were carried out on a 7.0T MRI (Bruker-Biospin). The tail vein was cannulated for injection of contrast agent. DCE-MRI was performed using a coronal T_1-weighted 3D gradient echo sequence (FLASH sequence, TR=67 ms, TE=3 ms, flip angle=70°, FOV=30×30 mm, imaging matrix=128×128, slice thickness=2.5 mm, 120 dynamic images, time interval=6.0s). For T_1 mapping, five pre-contrast scans were acquired with the same post-contrast parameters, but only a different flip angle (5°, 15°, 35°, 60°, and 70°). Baseline images were acquired for approximately 60 s (10 dynamic images), followed by an automatic injection over 4~5s of 0.1 mmol/kg Dotarem *via* mouse tail vein, followed by further acquisitions, up to a total time of 12 min (120 dynamic images).

Computer Simulations: The ideal AIF was modeled as a bi-exponential form (*3*). The simulated AIF was created based on noise level and scaling factor. The noise level is defined as percent signal change of peak value of the ideal AIF, and the scaling factor is defined as a ratio of peak value in a given voxel to peak value of the ideal AIF.

Automatic Detection of AIFs: The basic idea behind our method is that we can reduce the search space for possible AIF from voxel space into cluster space using clustering analysis (KCC); the AIF cluster was then determined among the candidate clusters based on the characteristics of concentration profiles in a cluster-by-cluster manner, rather than a voxel-by-voxel manner. Kendall's W was assigned to a given voxel by calculating the concentration time curves of this voxel with those of its nearest neighbor voxels (8 nearest neighbor voxels) (*4*). The KCC map was created using Kendall's W for all voxels. The regional homogeneity (ReHo) map was computed by thresholding the KCC map for finding candidate AIF clusters. The mean concentration profile was extracted by averaging concentration time curves across all voxels, which belong to each candidate AIF cluster. Characteristics of concentration profile such as before arrival time (BAT), time-to-peak (TTP), and the wash-in slope, were analyzed to find AIF cluster among candidate AIFs based on the assumption that the AIF has early arrival time, high peak value, and quick wash-in.

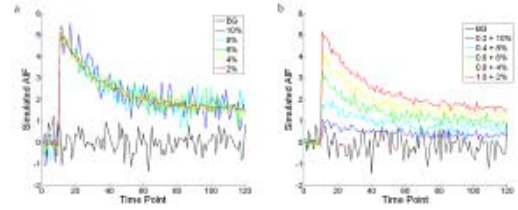

Fig. 1. Computer simulations of AIF. (a) Simulated AIF for different noise levels. (b) Simulated AIF for a combination of noise levels and scaling

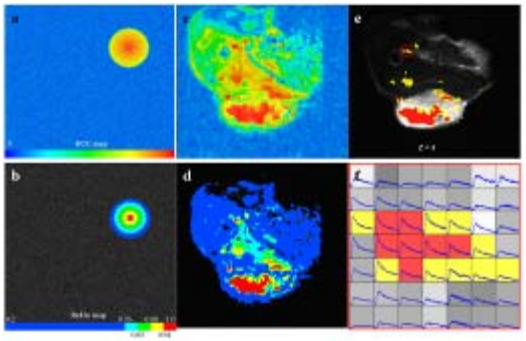

Fig. 2. KCC and ReHo map from computer simulations and mouse DCE-

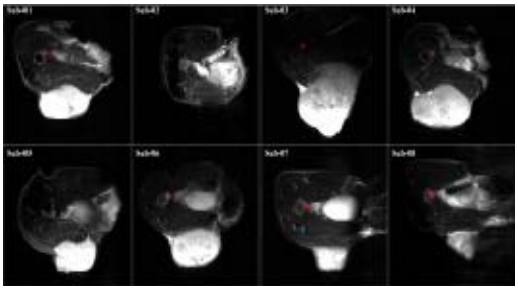

Fig. 3. Automatic detection of AIF for 8 mice DCE-MRI data.

Results

Results from Computer Simulations: Fig. 1 shows the computer simulations of AIF in aspect of noise levels and scaling factors. Figs. 2a and 2b show the simulated dynamic images at peak time point, the KCC map and ReHo map for the computer simulations of noise level and scaling factor. Results from KCC and ReHo map demonstrated that the Kendall's W decreased as voxels moved from central to peripheral regions, suggesting that the Kendall's W could provide the ability to locate regional homogeneous areas in aspects of noise levels and scaling factors.

Results from mouse DCE-MRI: To examine the feasibility of Kendall's W for automatic detection of the AIF, we applied our method to mouse DCE-MRI data. Figs. 2c and 2d show the KCC, ReHo map and candidate AIF cluster from one example taken from mouse DCE-MRI data. Fig. 2f shows the concentration profiles for each voxel within one cluster, which is defined as AIF cluster using our method (a red box in Fig. 2e). We tested our method for reproducibility across 8 mice. The AIF voxels were automatically detected near femoral arterial vessels across 8 mice (Fig 3). We found that the proposed method demonstrated robust detection of arterial vessels near the femoral artery in thigh tumor-bearing mouse images, which did not include images of the left ventricle of the heart. Permeability parameters estimated using our method were comparable with those using the manual determination of AIF in K^{trans} (8.85 ± 9.49 %), v_e (4.65 ± 2.34 %), and k_{ep} (11.72 ± 6.70 %), except for v_p (98.37 ± 739.11 %)

Discussion

In this study, we developed an automatic detection method for AIF that can be effective for use with mice data. Clusters for the potential AIF were created using the Kendall's coefficient of concordance (KCC), and then the characteristics of the concentration profile for each candidate cluster were examined for automatic detection of the AIF. We tested our proposed method using computer simulations and DCE-MRI data from mice. This facile and objective method for detection of AIF will greatly facilitate DCE-MRI in both clinical and pre-clinical assessment of angiogenesis for diagnosis and monitoring of therapeutic responses in cancer.

References

1. J. R. Garbow, A. C. Santeford, J. R. Anderson, J. A. Engelbach, J. M. Arbeit, *Cancer Res* 69, 7945 (Oct 15, 2009). **2.** S. Pickup, R. Zhou, J. Glickson, *Acad Radiol* 10, 963 (Sep, 2003). **3.** P. Wedeking *et al.*, *Magn Reson Imaging* 8, 567 (1990). **4.** M. Kendall, J. D. Gibbons, *Rank Correlation Methods*. (Oxford *Univ. Press, Oxford, 1990).*